

# Estimation of Time-Varying Ankle Joint Stiffness Under Dynamic Conditions via System Identification Techniques

Alejandro Moya Esteban<sup>1</sup>, Ronald C. van 't Veld<sup>1</sup>, Christopher P. Cop<sup>1</sup>, Guillaume Durandau<sup>1</sup>, Massimo Sartori<sup>1</sup> and Alfred C. Schouten<sup>1,2</sup>

**Abstract**—An important goal in the design of next-generation exoskeletons and limb prostheses is to replicate human limb dynamics. Joint impedance determines the dynamic relation between joint displacement and torque. Joint stiffness is the position-dependent component of joint impedance and is key in postural control and movement. However, the mechanisms to modulate joint stiffness are not fully understood yet. The goal of this study is to conduct a systematic analysis on how humans modulate ankle stiffness. Time-varying stiffness was estimated for six healthy subjects under isometric, as well as quick and slow dynamic conditions via system identification techniques; specifically, an ensemble-based algorithm using short segments of ankle torque and position recordings. Our results show that stiffness had the lowest magnitude under quick dynamic conditions. Under isometric conditions, with fixed position and varying muscle activity, stiffness exhibited a higher magnitude. Finally, under slow dynamic conditions, stiffness was found to be the highest. Our results highlight, for the first time, the variability in stiffness modulation strategies across conditions, especially across movement velocity.

## I. INTRODUCTION

Humans have the capacity to adapt the mechanical properties of their limbs to enable natural physical interaction even in complex environmental conditions, such as walking on ice. The central nervous system uses a variety of feedback and feedforward control strategies to regulate limb mechanical properties. A better understanding of these control strategies would contribute to improving the functionality of robotic devices such as biomimetic prostheses or exoskeletons, which cannot replicate human limb mechanical dynamics yet [1]. Additionally, new insights into these neural control strategies would improve the assessment and management of neurological disorders, like stroke or spinal cord injury, which lead to abnormal limb mechanical properties [2].

Joint impedance determines the dynamic relation between joint displacement and torque, and comprises three main components: inertia, damping and stiffness. Joint stiffness is the position-dependent component of joint impedance and is key in postural control and movement. Replicating human joint stiffness adaptations poses a major challenge in the field of biomimetic robotics. Many studies focus on analyzing joint stiffness under static conditions at a certain operation point, i.e. constant joint position and muscle activation [3].

\*This work was supported by the Netherlands Organisation for Scientific Research (NWO), domain Applied and Engineering Sciences projects 14903 and 522234, and partly by the ERC Starting Grant INTERACT (803035).

<sup>1</sup>Department of Biomechanical Engineering, University of Twente, Enschede, The Netherlands

<sup>2</sup>Department of Biomechanical Engineering, Delft University of Technology, Delft, The Netherlands

However, these experimental results have shown that joint stiffness strongly depends on the operating point, thus joint stiffness is a time-varying (TV) property during movement.

The number of studies analyzing joint stiffness under dynamic conditions with volitional movement remains low; likely due to the lack of standardized methods and the difficulty of studying stiffness during movement. The challenge arises due to two main factors [4]. First, joint stiffness depends on several variables (such as neural and muscle activation, reflex activity, passive tissue properties, muscle fatigue or training levels [5]) which are highly coupled and change continuously throughout movements. Thus, joint stiffness is characterized by nonlinear behavior. Second, volitional movements are managed by feedback and feedforward pathways of the human central nervous system. Hence, closed-loop analysis is required, which is more complex than standard (open-loop) analysis methods used under static conditions or imposed movements.

Several studies used system identification techniques, which rely on perturbation signals and system input/output relations, to estimate properties such as joint stiffness. Specifically, ensemble-averaging techniques, which estimate TV variables by means of a large set of input/output realizations with the same underlying TV patterns, are actively used [4], [6], [7], [8]. Most of these ensemble-based approaches need a large amount of realizations of the same movement, typically between 500 and 800, to accurately estimate the desired system properties. This results in time-consuming experiments in which subjects tend to experience muscle fatigue. To reduce the number of realizations, the multisegment (MS) algorithm has been designed to combine ensemble- with time-averaging to analyze TV properties [9]. As such, the MS algorithm produces non-parametric stiffness estimates with a more feasible number of required realizations for human subject experiments.

To the best of our knowledge, there are no studies that systematically compare how ankle joint stiffness is modulated throughout diverse conditions. Here, we perform a systematic analysis on how humans modulate ankle stiffness across different conditions. We assess ankle stiffness under isometric and dynamic conditions. Importantly, under dynamic conditions, we also evaluate how stiffness modulation is affected by movement velocity. In the remainder of the paper, the term 'isometric' will refer to the condition in which the ankle position is held constant, yet muscle activation varies. 'dynamic' will refer to the conditions in which both, position and muscle activation vary during the trial.

## II. METHODS

### A. Subjects

Six healthy subjects (5 male,  $24 \pm 1$  years) participated in the study. The protocol was approved by University of Twente ethics board, and all participants gave written informed consent.

### B. Apparatus

Ankle stiffness was measured using the Achilles Rehabilitation Device (MOOG, Nieuw-Vennep, The Netherlands), a one degree of freedom ankle manipulator, see Fig. 1. The Achilles applied small rotational displacements to the ankle in the sagittal plane, while recording angle and torque with a sampling frequency of 2048 Hz, both positive in dorsiflexion direction.

Electromyography (EMG) of the tibialis anterior (TA), soleus (SOL) and gastrocnemius lateralis (GL) muscles were recorded to obtain information about muscle activation patterns. EMG electrode placement was based on SENIAM guidelines [10]. EMG activity was recorded with a Porti system (TMSi, Oldenzaal, The Netherlands) at 2048 Hz.

### C. Experimental protocol

The experiment started with a recording of the maximum voluntary contraction (MVC) for all studied muscles. Then, subjects completed tasks in three different conditions, see Table I. The order in which subjects performed each condition was randomly pre-allocated, such that every possible order was completed by one of the six participants. Subjects completed a specific number of 2-minute trials per condition, see Table I. The required number of trials per condition was determined in a simulation study, which indicated that 250 sinusoidal realizations were adequate to estimate joint stiffness reliably. Subjects were given 2-minute rest periods between trials to minimize muscle fatigue.

Under dynamic conditions, the Achilles was regulated by an admittance controller, see Fig. 2. The controller created a

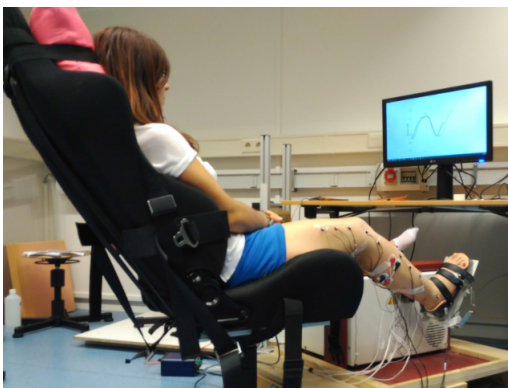


Fig. 1. Subjects were seated on a chair with their right foot strapped to the Achilles footplate using Velcro. The chair was positioned such that the knee angle was approximately 45 degrees with respect to the fully extended position. The ankle joint and motor axis were visually aligned, enabling plantarflexion and dorsiflexion movements. The initial ankle angle was set to 90 degrees. Visual feedback on both measured and target ankle torque (or angle) was provided on a monitor in front of the subject.

TABLE I  
MAIN CHARACTERISTICS OF THE THREE CONDITIONS

Task	Amplitude	Freq. [Hz]	Trials [#]	Duration [min]
Isometric	5 Nm	0.8	4	8
Dynamic	0.15 rad	0.6	6	12
Dynamic	0.15 rad	0.3	11	22

virtual environment dictated by three virtual parameters: inertia, damping and stiffness. The controller virtual parameters were chosen so that the actuator offered resistance against the movement, but not excessively, to prevent fatigue: inertia =  $1 \text{ kg}\cdot\text{m}^2$ , damping =  $2.5 \text{ Nm/rad/s}$  and stiffness =  $60 \text{ Nm/rad}$ . For the dynamic task, subjects were instructed to oscillate their ankle position by tracking a 0.6 or 0.3 Hz target sine with a magnitude of  $\pm 0.15$  radians around the initial ankle angle. Under the isometric condition, the manipulator was position controlled and subjects were instructed to exert a torque by tracking a 5 Nm amplitude target sine at a rate of 0.8 Hz, while the ankle angle was fixed to 90 degrees. In all conditions, the Achilles device added a small pseudo-random binary sequence (PRBS) displacement perturbation. The amplitude of the perturbation was 0.03 radians and its switching time was set to 0.15 seconds.

### D. Data analysis

EMG signals were processed to obtain EMG linear envelopes. Raw signals were: bandpass filtered (bandpass frequency: 30-300 Hz), full-wave rectified and low-pass filtered (cut-off frequency: 6 Hz). All filters were zero-lag 2<sup>nd</sup> order Butterworth filters. MVC data were used to normalize the linear envelopes.

An extended version of the multisegment (MS) algorithm was used to estimate TV ankle stiffness in closed-loop conditions [6], [9]. The MS algorithm requires ensembles of data with the same underlying TV behavior. Hence, the algorithm is optimal for periodic signals, such as sinusoidal waves. The MS algorithm computes double-sided estimates of the impulse response function (IRF) of the system by means of auto- and cross-correlation functions. The estimation of ankle joint stiffness from position, torque and perturbation signals

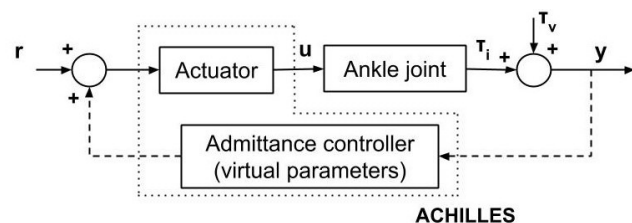


Fig. 2. Schematic of Achilles controller. Under dynamic conditions, subjects had to produce a voluntary torque,  $\tau_v$ , to track the target sinusoid. The measured torque,  $y$ , consists of this voluntary torque together with the torque in response to the ankle motion,  $\tau_i$ . The admittance model of the virtual environment transforms this total torque in the desired (unperturbed) ankle position. The actuator adds the perturbation signal,  $r$ , to generate the final ankle position,  $u$ . Under the isometric condition, the admittance controller is absent (symbolized with dashed arrows).

involves several processing steps: segmentation of individual sinusoidal realizations, minimization of variability across realizations (through an alignment algorithm and outlier removal) and removal of the ensemble mean to exacerbate perturbation-induced response. These steps are described in detail in previous studies [6].

To check the statistical validity of the MS algorithm, a bootstrap algorithm was implemented. The bootstrapping consisted of randomly choosing 95% of the realizations in the ensemble to estimate stiffness. This process was repeated a total of 35 times to obtain the mean and standard deviation of the estimated stiffness. A larger number of repetitions did not result in lower standard deviation.

### III. RESULTS

Ankle joint stiffness was modulated during all conditions, see Fig. 3(a)-(c). In each condition, the subject experienced two periods of increased stiffness: one during ankle dorsiflexion (DF), or positive ankle torque, and one during plantarflexion (PF), or negative ankle torque. Maximum stiffness peaks were followed by low stiffness periods, which were related to the transition between DF and PF (and vice versa). In these transitions, the net torque exerted by subjects was 0 Nm.

For the same subject as Fig. 3, the percentage of the cycle in which torque and stiffness maximum and minimum peaks appeared, together with the peak value, are listed in Table II. Stiffness minimum peaks following PF and DF phases are listed as “PF stiffness min. peak” and “DF stiffness min. peak”, respectively. Note that torque minimum peaks are always located at 0 or 100% of the cycle due to the segmentation of the individual sinusoidal realizations. Under isometric and quick dynamic (0.6 Hz) conditions,

the torque peaks closely matched the timing of the stiffness peaks in DF and PF. However, under slow dynamic (0.3 Hz) condition, stiffness peaks appeared to be shifted forward in the cycle with respect to torque peaks. The torque transitions between DF and PF (and vice versa) coincided with stiffness minimum peaks. Again, a forward shift between minimum stiffness peaks and zero-torque points is observed for slow dynamic condition. Under isometric conditions, the stiffness minimum peak following PF was also shifted with respect to the zero-torque point.

The highest absolute stiffness peak values, for both PF and DF, were observed under slow dynamic condition, followed by isometric and quick dynamic conditions, see Table II.

TABLE II  
CYCLE LOCATION AND VALUE OF TORQUE, STIFFNESS AND EMG  
EVENTS FOR REPRESENTATIVE SUBJECT. STANDARD DEVIATIONS ARE  
LISTED IN PARENTHESIS.

Event		Isometric	Dynamic 0.6 Hz	Dynamic 0.3 Hz
Torque	[% cycle]	100	100	0
min. peak	[Nm]	-5.9 (1.0)	-7.7 (1.0)	-8.6 (1.1)
0Nm Torque	[% cycle]	20 (4)	20 (5)	24 (4)
Torque	[% cycle]	48 (7)	50 (4)	50 (5)
max. peak	[Nm]	5.2 (0.9)	7.5 (1.0)	7.9 (0.9)
0Nm Torque	[% cycle]	73 (5)	71 (5)	74 (4)
PF stiffness	[% cycle]	2 (1)	97 (1)	11 (1)
max. peak	[Nm/rad]	23.7 (0.8)	20.4 (0.8)	31.9 (1.4)
PF stiffness	[% cycle]	36 (2)	29 (1)	41 (1)
min. peak	[Nm/rad]	10.4 (0.8)	3.7 (0.8)	15.4 (0.9)
DF stiffness	[% cycle]	48 (1)	52 (1)	61 (1)
max. peak	[Nm/rad]	16.5 (0.8)	10.5 (0.9)	21.9 (1.2)
DF stiffness	[% cycle]	73 (1)	73 (1)	83 (1)
min. peak	[Nm/rad]	11.0 (0.6)	4.0 (0.9)	13.4 (0.7)
TA EMG	[% cycle]	35 (11)	43 (8)	46 (6)
max. peak	[-]	0.12 (0.03)	0.18 (0.04)	0.18 (0.04)
SOL EMG	[% cycle]	82 (12)	94 (7)	99 (4)
max. peak	[-]	0.07 (0.01)	0.14 (0.04)	0.20 (0.05)
GL EMG	[% cycle]	83 (7)	88 (6)	96 (13)
max. peak	[-]	0.15 (0.04)	0.25 (0.05)	0.16 (0.04)

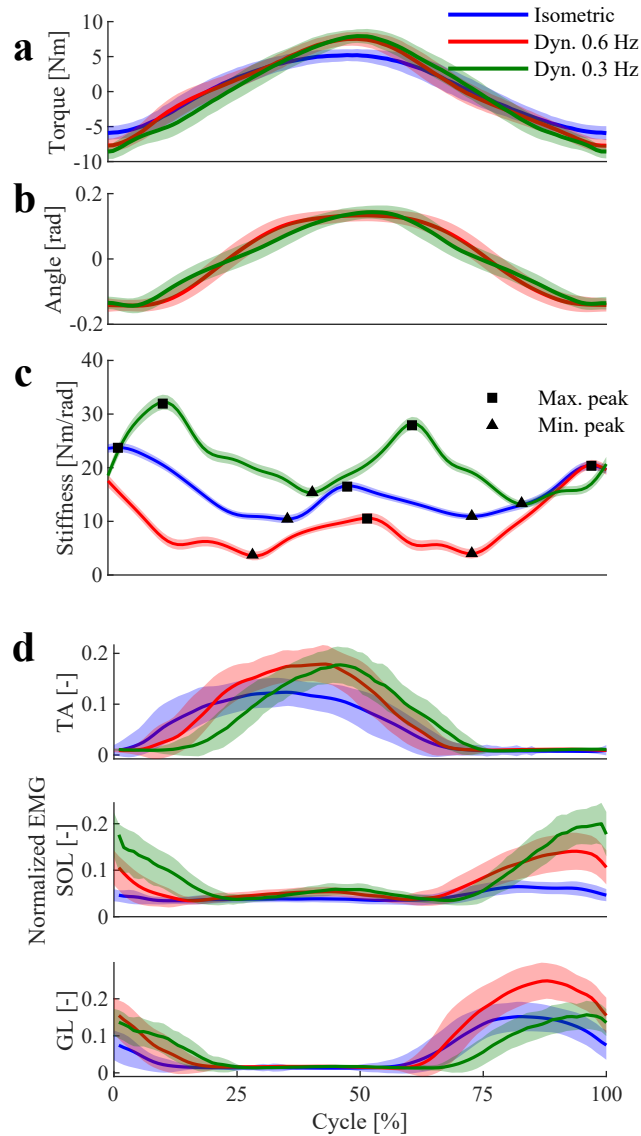


Fig. 3. (a) Measured torque. Solid lines show the ensemble mean; (b) Measured ankle angle. The initial ankle angle was subtracted, thus, positive angle means DF, and negative, PF; (c) Estimated stiffness for the three conditions. Solid line corresponds to the mean estimated stiffness over 35 repetitions of the MS algorithm; (d) Normalized EMG activity for the three conditions and TA, SOL and GL. The shaded areas correspond to  $\pm 1$  standard deviation. Data is from a representative subject.

The aforementioned trend was not observed for minimum and maximum torque peaks. The largest absolute torque peak values appeared during slow dynamic condition, followed by quick dynamic and isometric conditions.

Fig. 3(d) shows normalized EMG activity for ankle plantarflexors (GL and SOL) and dorsiflexor (TA). Table II shows the cycle location of the EMG peak and its value. As expected, the EMG maximum peaks were always given before the torque peaks and the maximum stiffness peak.

#### IV. DISCUSSION

The goal of the present study was to conduct, for the first time, a systematic and comprehensive analysis on how humans modulate ankle joint stiffness across different conditions, specially across movement velocity. Three conditions were analyzed: isometric, quick and slow dynamic, at movement frequencies of 0.8, 0.6 and 0.3 Hz, respectively. We found TV ankle stiffness during quick dynamic conditions to exhibit the lowest magnitude. These results are in accordance with previous studies, focused on the knee [4], [6] and elbow joints [11]. These studies have shown that stiffness during movements is lower than under static and isometric conditions. Two factors may contribute to the lower stiffness under quick dynamic conditions. First, reduced muscle stretch reflexes during movement. IRFs used to estimate stiffness in the present study are long enough (117 ms) to include stretch reflexes. Stretch reflexes can account for half of the torque response elicited by perturbations [12]. Stretch reflexes are around 25% smaller during dynamic tasks compared with tasks with constant position and muscle activation [6]. Second, passive muscle stiffness is reduced during movements, as muscles operate outside of short-range stiffness limits [6], [13]. At the knee joint, passive joint stiffness is reduced around 20% during sinusoidal movement, compared with isometric tasks [6].

Under isometric conditions, ankle stiffness exhibited a higher magnitude compared with quick dynamic conditions. This was expected due to the lack of joint movement during isometric conditions. The higher magnitude suggests that, in postural tasks, increasing stiffness is a valid strategy to cope with external disturbances. However, slow dynamic conditions presented the highest stiffness. Preventing perturbation-induced deviations while performing a slow movement was regarded as a demanding task by subjects, which may explain the increased stiffness. However, substantial differences in muscle activation patterns across conditions were not found. This suggests that other factors must have influenced ankle stiffness. Moreover, despite the consistency in muscle activation patterns (across subjects and conditions), the estimated stiffness shows much more variability. The lack of consistency in estimated stiffness may be explained by differences across conditions, in properties such as reflexes, muscle force-length and force-velocity relationships, pennation angle or moment arms. Musculoskeletal models such as EMG-driven models may provide insight in the physiological changes of the aforementioned properties [14].

From studies with constant muscle activation and position, it is well known that joint stiffness scales with muscle activation [3]. During isometric condition, the minimum stiffness was found at the torque transitions from PF to DF (and vice versa). This drop is likely caused by the switch between the activation of ankle dorsiflexors and plantarflexors [4]. During slow dynamic condition, we also observed that, for every subject, stiffness peaks (maximum and minimum) were shifted forward in the cycle with respect to ankle torques. The shift was consistent for all maximum and minimum stiffness peaks. Such behavior is in accordance with previous studies [4], which found that stiffness peaks did not correlate with torque peaks during volitional movements.

The ultimate goal of this research is to be able to replicate human stiffness modulation strategies in robotic devices. Despite limitations such as a small range of velocities, and lack of comparison with other algorithms for stiffness estimation, our study lays the foundation for future work since we obtained primary results on a relatively unexplored behavior: velocity-dependent ankle stiffness modulation.

#### REFERENCES

- [1] A. H. Hansen, D. S. Childress, S. C. Miff, S. A. Gard, and K. P. Mesplay, "The human ankle during walking: implications for design of biomimetic ankle prostheses," *J. Biomech.*, vol. 37, no. 10, pp. 1467–1474, 2004.
- [2] M. Mirbagheri, H. Barbeau, M. Ladouceur, and R. Kearney, "Intrinsic and reflex stiffness in normal and spastic, spinal cord injured subjects," *Exp. Brain Res.*, vol. 141, no. 4, pp. 446–459, 2001.
- [3] G. L. Gottlieb and G. C. Agarwal, "Dependence of human ankle compliance on joint angle," *J. Biomech.*, vol. 11, pp. 177–181, 1978.
- [4] D. Ludvig and E. J. Perreault, "Task-relevant adaptation of musculoskeletal impedance during posture and movement," in *Proc. Am. Control Conf.*, June 2014, pp. 4784–4789.
- [5] G. Durandau, D. Farina, and M. Sartori, "Robust real-time musculoskeletal modeling driven by electromyograms," *IEEE Trans. Biomed. Eng.*, vol. PP, pp. 1–1, May 2017.
- [6] D. Ludvig, M. Plocharski, P. Plocharski, and E. J. Perreault, "Mechanisms contributing to reduced knee stiffness during movement," *Exp. Brain Res.*, vol. 235, no. 10, pp. 2959–2970, 2017.
- [7] E. J. Rouse, L. J. Hargrove, E. J. Perreault, and T. A. Kuiken, "Estimation of human ankle impedance during the stance phase of walking," *IEEE Trans. Neural Syst. Rehabil. Eng.*, vol. 22, no. 4, pp. 870–878, Jul. 2014.
- [8] H. Lee and N. Hogan, "Time-varying ankle mechanical impedance during human locomotion," *IEEE Trans. Neural Syst. Rehabil. Eng.*, vol. 23, no. 5, pp. 755–764, Sep. 2015.
- [9] D. Ludvig and E. J. Perreault, "System identification of physiological systems using short data segments," *IEEE Trans. Biomed. Eng.*, vol. 59, no. 12, pp. 3541–3549, 2012.
- [10] D. Stegeman and H. Hermens, "Standards for surface electromyography: The european project surface EMG for non-invasive assessment of muscles (SENIAM)," vol. 1, Jan. 2007.
- [11] D. Bennett, J. Hollerbach, Y. Xu, and I. Hunter, "Time-varying stiffness of human elbow joint during cyclic voluntary movement," *Exp. Brain Res.*, vol. 88, no. 2, pp. 433–442, 1992.
- [12] N. Mrachacz-Kersting and T. Sinkjær, "Reflex and non-reflex torque responses to stretch of the human knee extensors," *Exp. Brain Res.*, vol. 151, no. 1, pp. 72–81, 2003.
- [13] R. Kearney and I. Hunter, "Dynamics of human ankle stiffness: variation with displacement amplitude," *J. Biomech.*, vol. 15, no. 10, pp. 753–756, 1982.
- [14] C. P. Cop, G. Durandau, A. Moya Esteban, R. C. van 't Veld, A. C. Schouten, and M. Sartori, "Model-based estimation of ankle joint stiffness during dynamic tasks: a validation-based approach," *41st Annual International Conference of the IEEE Engineering in Medicine Biology Society (EMBC)*, Jul. 2019.